# The Role of Antibody Polyspecificity and Lipid Reactivity in Binding of Broadly Neutralizing Anti-HIV-1 Envelope Human Monoclonal Antibodies 2F5 and 4E10 to Glycoprotein 41 Membrane Proximal Envelope Epitopes[1]

**S. Munir Alam,[2]* Mildred McAdams,* David Boren,* Michael Rak,* Richard M. Scearce,* Feng Gao,* Zenaido T. Camacho,* Daniel Gewirth,[3]* Garnett Kelsoe,* Pojen Chen,[†] and Barton F. Haynes[2]***

**Two neutralizing human mAbs, 2F5 and 4E10, that react with the HIV-1 envelope gp41 membrane proximal region are also polyspecific autoantibodies that bind to anionic phospholipids. To determine the autoantibody nature of these Abs, we have compared their reactivities with human anti-cardiolipin mAbs derived from a primary antiphospholipid syndrome patient. To define the role of lipid polyreactivity in binding of 2F5 and 4E10 mAbs to HIV-1 envelope membrane proximal epitopes, we determined the kinetics of binding of mAbs 2F5 and 4E10 to their nominal gp41 epitopes vs liposome-gp41 peptide conjugates. Both anti-HIV-1 mAbs 2F5 and 4E10 bound to cardiolipin with $K_d$ values similar to those of autoimmune anti-cardiolipin Abs, IS4 and IS6. Binding kinetics studies revealed that mAb 2F5 and 4E10 binding to their respective gp41 peptide-lipid conjugates could best be defined by a two-step (encounter-docking) conformational change model. In contrast, binding of 2F5 and 4E10 mAbs to linear peptide epitopes followed a simple Langmuir model. A mouse mAb, 13H11, that cross-blocks mAb 2F5 binding to the gp41 epitope did not cross-react with lipids nor did it neutralize HIV-1 viruses. Taken together, these data demonstrate the similarity of 2F5 and 4E10 mAbs to known anti-cardiolipin Abs and support the model that mAb 2F5 and 4E10 binding to HIV-1 involves both viral lipid membrane and gp41 membrane proximal epitopes.** ***The Journal of Immunology,*** **2007, 178: 4424–4435.**

Human mAbs 2F5 and 4E10 are two rare broadly neutralizing Abs that interact with the membrane proximal external region (MPER)[4] of the HIV-1 gp41 segment of HIV-1 envelope (Env) (1–4). mAbs 2F5 and 4E10 bind to conserved core amino acid residues ELDKWA and NWFDIT, respectively, that lie outside the six-helix bundle structures of the heptad repeat region of gp41 (5–8). Both nominal peptide epitopes and soluble recombinant Env gp160 proteins that include the MPER 2F5 and 4E10 epitopes fail to generate broadly reactive neutralizing Abs after immunization of animals and humans (9, 10). mAbs 2F5 and 4E10 are both unusual in that they have long, hydrophobic Ig CDR3 regions (11–14).

We have recently determined the reactivity of mAbs 2F5 and 4E10 with human autoantigens and found reactivity of mAb 2F5 with Ro (Sjogren's syndrome Ag), histones, centromere B, and cardiolipin (15). mAb 4E10 reacted with Ro (Sjogren's syndrome Ag), centromere B, and cardiolipin as well as other phospholipids such as phosphatidylserine. In addition, mAb 4E10 had lupus anticoagulant activity with prothrombin reactivity, resulting in prolongation of the partial thromboplastin time (15). Based on the crystal structures of mAbs 2F5 and 4E10, it has been proposed that the long, hydrophobic CDR3 loops of both 2F5 and 4E10 mAbs might interact with a lipid component on the viral surface, because only small regions of both mAb CDR3 interacted with the antigenic peptide, leaving large hydrophobic CDR3 components to interact with the virion membrane (1, 2). The presence of long hydrophobic CDR3 regions and the observation of direct binding of broadly neutralizing mAbs 2F5 and 4E10 to lipid autoantigens have prompted the hypothesis that anti-HIV-1 Abs like 2F5 and 4E10 are rarely made due to B cell tolerance mechanisms (15–20).

Anti-phospholipid Abs that include Abs against the anionic phospholipid, cardiolipin, can be associated with recurrent thrombosis in patients with the antiphospholipid syndrome (APS) (21, 22). Nonpathogenic anti-cardiolipin Abs can also be found in patients with a variety of infectious diseases due to disordered immunoregulation, including HIV-1, syphilis, and leishmaniasis (23). APS patients make anti-cardiolipin Abs that bind to a variety of phospholipids and cofactors, with pathogenicity of those Abs being associated with Ab reactivity with $\beta$-2-glycoprotein-1 (24, 25). In general, anti-phospholipid mAbs from APS patients contain

*Department of Medicine, Duke University School of Medicine, Durham, NC 27710; and [†]Department of Medicine, University of California, Los Angeles, CA 90095

Received for publication November 15, 2006. Accepted for publication January 12, 2007.

The costs of publication of this article were defrayed in part by the payment of page charges. This article must therefore be hereby marked *advertisement* in accordance with 18 U.S.C. Section 1734 solely to indicate this fact.

[1] This work was supported by the National Institutes of Health Center for HIV/AIDS Vaccine Immunology Grant, AI0678501, by National Institute of Allergy and Infectious Diseases P01 AI52816, AI51445, and a Collaboration for AIDS Vaccine Discovery grant from the Bill and Melinda Gates Foundation.

[2] Address correspondence and reprint requests to Dr. Barton F. Haynes, Duke Human Vaccine Institute, Box 3258, Duke University, RP1 Circuit Drive, Room 107, Durham, NC 27710; E-mail address: hayne002@mc.duke.edu or Dr. S. Munir Alam, Duke Human Vaccine Institute, Box 3258, Duke University, RP1 Circuit Drive, Room 107, Durham, NC 27710; E-mail address: alam0004@mc.duke.edu

[3] Current address: Hauptman-Woodward Medical Research Institute, Buffalo, NY 14203.

[4] Abbreviations used in this paper: MPER, membrane proximal external region; Env, envelope; APS, antiphospholipid syndrome; SPR, surface plasmon resonance; RU, response unit; SA, streptavidin; HR, heptad repeat.

large numbers of somatic mutations in their $V_H$ and $V_L$ sequences, with arginine residues in their CDR3 region (26–28).

In this study, we demonstrated that the kinetics of mAbs 2F5 and 4E10 binding to cardiolipin are similar to typical anti-APS cardiolipin autoantibodies. In addition, we have characterized the reactivity of mAbs 2F5 and 4E10 with gp41 membrane proximal epitopes in the context of synthetic liposomes and showed that the mAbs 2F5 and 4E10 mAbs dock onto gp41-derived peptides anchored in synthetic liposome membranes in a conformational change model, thereby positioning the mAbs for high-affinity binding to the HIV-1 gp41 membrane proximal region.

## Materials and Methods

### *Antibodies*

Anti-HIV-1 gp41 (antimembrane proximal) mAbs 2F5 and 4E10 (3) were purchased from Polymun. Anti-cardiolipin mAbs IS4 and IS6 were derived from an APS patient and hybridomas and were generated as described (29). The CD4 inducible anti-HIV-1 gp120 mAb 17b (30, 31) was provided by Dr. J. Robinson (Tulane University, New Orleans, LA). Fab of mAb 2F5 were the gift of P. Kwong, R. Wyatt, and G. Ofek (Vaccine Research Center, National Institutes of Health, Bethesda, MD) (1). Fab of mAb 4E10 were the gift of D. Burton, I. Wilson, and R. Cardoso (The Scripps Research Institute, La Jolla, CA) (2). Both Fab Ab reagents were analyzed on a Superdex HR200 column and found to be free of dimer forms. Mouse mAb 13H11 was produced from splenocytes from a mouse immunized with HIV-1 Env oligomer CON-S (32), as described (33). All mAbs were purified by affinity chromatography on anti-Ig columns.

### *Proteins*

rHIV-1 Env gp140 proteins, CON6 gp140, CON-S gp140, and JRFL gp140 were produced using recombinant vaccinia viruses and purified as described (10, 32, 34). BSA, OVA was purchased from Sigma-Aldrich.

### *Peptides*

Peptides were synthesized (SynPep) and purified by reverse-phase HPLC. Purity of the peptides were assessed by HPLC to be >95% and confirmed by mass spectrometric analysis. Peptides used in this study include the following: HIV-1 gp41 2F5 epitope peptides, $2F5_{663-677}$ (NEQELLELD KWASLWSGGRGG-biotin), GTH1–$2F5_{659-678}$ (YKRWIILGLNKIVR MYSQQEKNEQELLELDKWASLWN-biotin), and HIV-1 gp41 4E10 epitope peptides, $4E10_{675-690}$ (SLWNWFNITNWLWYIK), and GTH1–$4E10_{675-690}$ (YKRWIILGLNKIVRMYSSLWNWFNITNWLWYIK). Randomly scrambled sequences of the above peptides were used as controls. Full-length HR-2 gp41 peptide (DP178), YTSLIHSLIEESQNQQQEKNEQELL ELDKWASLWNF, while the HR-1 peptide (DP107), NNLLRAIEAQQHL LQLTVWGIKQLQARILAVERYLKDQ, was used as a control.

### *Phospholipids*

Phospholipids 1-palmitoyl-2-oleoyl-*sn*-glycero-3-phosphatidylcholine (POPC), 1-palmitoyl-2-oleoyl-*sn*-glycero-3-phosphatidylserine (POPS), 1,2-dioleoyl-*sn*-glycero-3-phosphatidylserine (DOPS), 1-palmitoyl-2-oleoyl-*sn*-glycero-3-phosphatidylethanolamine (POPE), 1,2-dioleoyl-*sn*-glycero-3-phosphatidylethanolamine (DOPE); cardiolipin (heart cardiolipin), 1,2-dimyristoyl-*sn*-glycero-3-phosphate (DMPA), and cholesterol dissolved in chloroform were purchased from Avanti Polar Lipids.

### *Preparation of aqueous phospholipid suspension and liposomes*

Phospholipid liposomes were prepared by dispensing appropriate molar amounts of phospholipids in chloroform-resistant tubes. The phospholipids were mixed by gentle vortexing and the mixture was dried in the fume hood under a gentle stream of nitrogen. Any residual chloroform was removed by storing the lipids under a high vacuum (15 h). Aqueous suspensions of phospholipids were prepared by adding PBS or TBS buffer (pH 7.4) and kept at a temperature above the transition temperature for 10–30 min, with intermittent, vigorous vortexing to resuspend the phospholipids. The milky, uniform suspension of phospholipids was then sonicated in a bath sonicator (Misonix Sonicator 3000). The sonicator was programmed to run three consecutive cycles of 45 s of total sonication per cycle. Each cycle included 5 s of sonication pulse (70 W power output) followed by a pulse off period of 12 s. At the end of sonication, the suspension of lamellar liposomes was stored at 4°C and was thawed and sonicated again as described above before capture on BIAcore sensor chip. POPC:POPS and POPC:cardiolipin liposomes were prepared by mixing the phospholipids at molar ratios of 3:1 (POPC:POPS or POPC:cardiolipin).

### *Anchoring of membrane proximal peptides to synthetic liposomes*

To design peptides that would associate with the outer layer of liposomes, we synthesized membrane proximal 2F5 and 4E10 nominal epitopes with a HIV-1 p24 gag $\alpha$-helix region (GTHI) YKRWIILGLNKIVRMYS, N-terminal to the membrane proximal epitopes. In preliminary experiments, we have previously shown this peptide design facilitates peptide interaction with lipid bilayers via the GTHI peptide (B. F. Haynes, A. M. Moody, S. M. Alam, unpublished observations). HIV-1 membrane proximal peptides GTH1–$2F5_{656-670}$ and GTH1–$4E10_{675-690}$ were dissolved in 70% chloroform, 30% methanol. Chloroform solutions of lipids were added to the peptide solution, in molar ratios of 45:25:20:10 (POPC:POPE:DMPA: cholesterol). Each peptide was added to a molar ratio of peptide:total phospholipids of 1:420. The mixture was vortexed, then dried and resuspended as described above.

### *Surface plasmon resonance (SPR) measurements*

All SPR measurements were conducted on a BIAcore 3000 instrument and data analyses were performed using the BIAevaluation 4.1 software (BIAcore). Specific binding assays for rate constants and equilibrium $K_d$ measurements were performed as described below.

***Kinetics and affinity of mAb binding to peptide epitopes.*** Biotinylated versions of 2F5 ($2F5_{656-670}$), GTH1–$4E10_{675-690}$ peptides, and scrambled sequences of 2F5 peptides were individually anchored on a BIAcore SA sensor chip as described earlier (35). Each peptide was injected until 100–150 response units (RU) of binding to streptavidin was observed. Specific binding responses of mAb binding were obtained following subtraction of nonspecific binding on the scrambled 2F5 peptide surface. Rate constants were measured using the Langmuir equation and global curve fitting to binding curves obtained from mAb titrations, which ranged from 0.01 to 119 nM and 6.0 to 1400 nM for mAbs 2F5 and 4E10, respectively. The mAbs were injected at 30 $\mu$l/min for 2–6 min and glycine-HCl (pH 2.0) and surfactant P20 (0.01%) were used as the regeneration buffer.

***Kinetics and affinity of mAb binding to phospholipids.*** Phospholipid-containing liposomes were captured on a BIAcore L1 sensor chip, which uses an alkyl linker for anchoring lipids. Before capturing lipids, the surface of the L1 chip was cleaned with a 60-s injection of 40 mM octyl $\beta$-D-glucopyranoside, at 100 $\mu$l/minute, and the chip and fluidics were washed with excess buffer to remove any traces of detergent. After each Ab injection, the surface was again cleaned with octyl $\beta$-D-glucopyranoside, and 5-s injections of each 5 mM HCl, then 5 mM NaOH, to clean any adherent protein off the chip.

In experiments to demonstrate specificity of mAb 4E10 and 2F5 binding to cardiolipin, cardiolipin was anchored to near saturation (~6000 RU) on one of the flow cells of the L1 sensor chip. On two of the remaining flow cells, OVA and BSA were immobilized using amine coupling chemistry to ~3000 RU. mAbs 17b, 2F5, and 4E10 were then injected at 100 $\mu$g/ml at a flow rate of 30 $\mu$l/min. For kinetics and affinity measurements of mAb binding to cardiolipin, BSA was immobilized to all flow cells with ~3000 RU of BSA. This step was important as we observed nonspecific binding of all mAbs to the blank L1 sensor surface and this level of nonspecificity was abrogated with chip coating with BSA. Second, to minimize rebinding and mass transfer, we immobilized cardiolipin at a predetermined optimal level of ~500 RU. The Biacore L1 sensor chip was used for anchoring cardiolipin, whereas a streptavidin (SA) sensor chip was used for peptide immobilization. In each binding assay, flow cell 1, with immobilized BSA but no cardiolipin, served as a control for nonspecific binding. For each cycle of binding, specific binding responses were calculated by in-line subtraction of responses from flow cell 1 (see Fig. 1). Global curve fitting to the Langmuir equation was used to derive rate constants and steady-state analysis for calculation of $K_d$. The two-step conformational change model ($A+B \rightarrow ABx$, (encounter step); $ABx \rightarrow AB$, (docking step)) was used for binding of MPER mAbs, 2F5 and 4E10, to peptide-lipid conjugates.

### *RNA isolation from hybridomas*

The IS6 hybridoma cells were lysed with the TRIzol reagent (Invitrogen Life Technologies). The total mRNA was isolated according to the manufacturer's protocol and resuspended in 20 $\mu$l of diethyl pyrocarbonate-treated $H_2O$.

### *Cloning of $\gamma$H and $\lambda$L chain V(D)J rearrangements from cDNA by RACE*

IS6 mRNA was used in a 5′ RACE reaction using the GeneRacer kit (Invitrogen Life Technologies) according to the manufacturer's protocol.

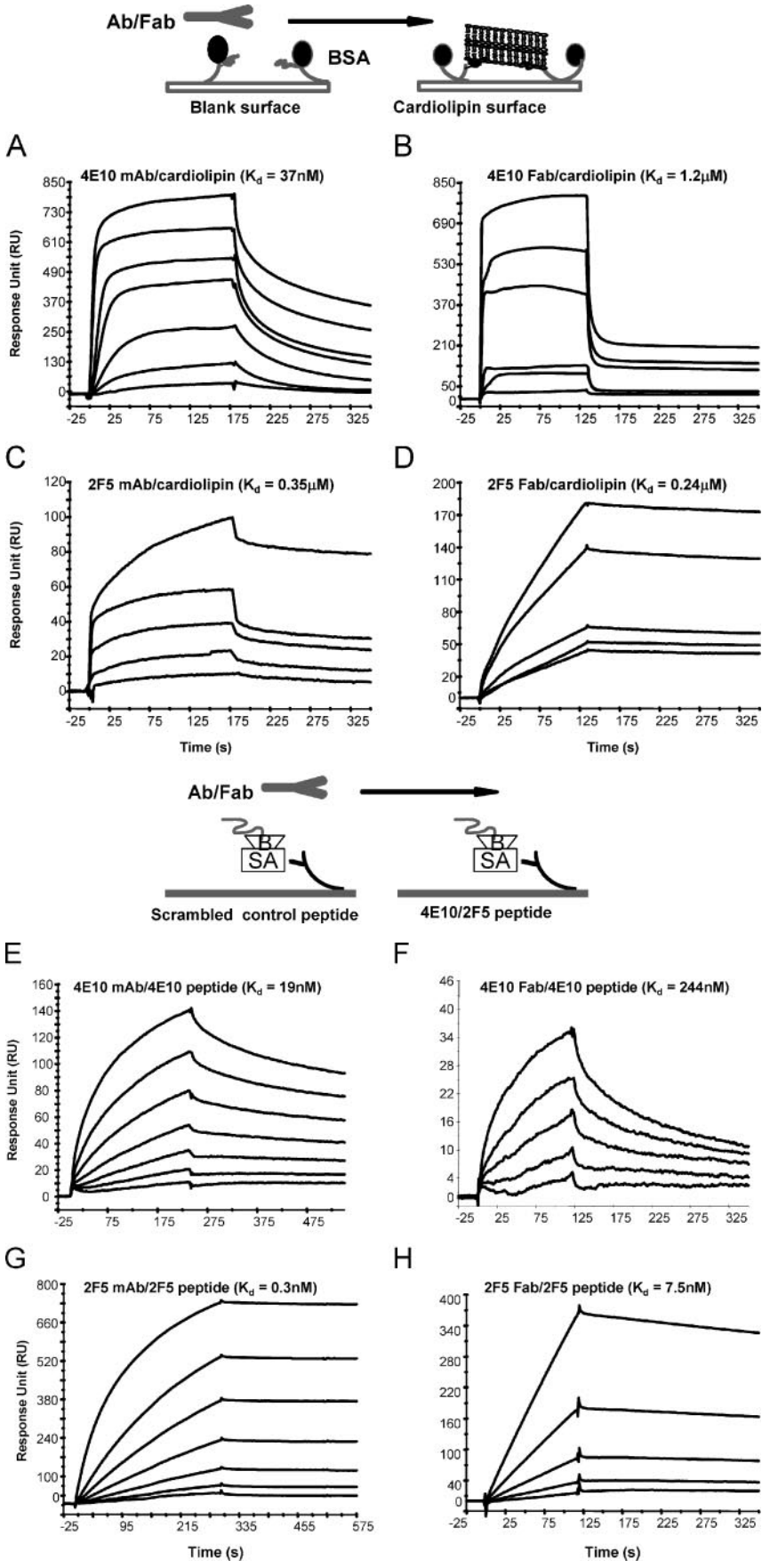


**FIGURE 1.** Binding of 4E10 and 2F5 mAb and Fab to cardiolipin and peptide epitopes. Approximately 400–600 RU of cardiolipin in an aqueous suspension was coupled to the BIAcore L1 sensor, on which ~3000 RU of BSA was immobilized previously. Whole mAb (*A*, *C*, *E*, and *G*) or Fab (*B*, *D*, *F*, and *H*) of either 2F5 or 4E10 was then injected at varying concentrations. The Ab concentration range used was as follows: 4E10 mAb (1.66–333 nM); 4E10 Fab (27.3–1800 nM); 2F5 mAb (46.6–1800 nM); 2F5 Fab (120–2000 nM). Due to the biphasic nature of binding, steady-state $K_D$ values were derived for 4E10 mAb and 4E10 Fab and 2F5 mAb, whereas $K_d$ values for 2F5 Fab were derived from kinetics rate constants. Data shown are specific binding of each mAb or Fab after subtraction of nonspecific signals over a BSA immobilized surface. For binding to peptide epitopes, ~150–200 RU of biotinylated peptides were immobilized to streptavidin that was coupled to a BIAcore sensor chip (SA). Whole mAb or Fab were then injected at varying concentrations, which were at 11–714 nM (4E10), and 0.156–5 nM (2F5) for whole mAb and 125–2000 nM (4E10) and 0.62–9.95 nM (2F5) for Fab.

Briefly, 5 $\mu$l of total mRNA was dephosphorylated with calf intestinal phosphatase, extracted with phenol and precipitated with ethanol. The mRNA was then uncapped with tobacco acid pyrophosphatase, extracted with phenol, and precipitated with ethanol. An RNA oligonucleotide provided in the kit was ligated to the 5′ end of the mRNA. After the ligation, the reaction was extracted with phenol, precipitated with ethanol, and

Table I. *Binding rate constants of anti-HIV-1 gp41 membrane proximal and anti-cardiolipin mAbs*[a]

| mAb/Ag | $k_a$ $\times 10^3$ $M^{-1}$ $s^{-1}$ | $k_d$ $\times 10^{-3}$ $s^{-1}$ | $K_d$ nM |
|---|---|---|---|
| 4E10 mAb/4E10 peptide | 63 ± 1.1 | 1.2 ± 0.1 | 20.2 ± 3.3 |
| 4E10 Fab/4E10 peptide | 40 ± 13.0 | 6.2 ± 2.4 | 255 ± 19.2 |
| 2F5 mAb/2F5 peptide | 633 ± 16.8 | 0.2 ± 0.01 | 0.27 ± 0.2 |
| 2F5 Fab/2F5 peptide | 287 ± 43 | 2.6 ± 0.8 | 9.0 ± 2.1 |
| 13H11 mAb/2F5 peptide | 488 ± 32.4 | 6.6 ± 1.6 | 12.4 ± 0.4 |
| 4E10 mAb/Con S gp140 | 108 ± 7.1 | 1.7 ± 0.3 | 160 ± 38.0 |
| 2F5 mAb/ConS gp140 | NA* | NA* | >1000 |
| IS6 mAb/Con S gp140 | 5.0 ± 1.9 | 3.0 ± 0.22 | 407 ± 86 |
| 2F5 mAb/JRFL gp140 | 3.6 ± 0.74 | 0.54 ± 0.03 | 164 ± 34.3 |
| 4E10 mAb/JRFL gp140 | 1.8 ± 0.2 | 1.95 ± 0.17 | 1090 ± 15.5 |
| 4E10 mAb/cardiolipin | NA | NA | 37 |
| 2F5 mAb/cardiolipin | NA | NA | 350 |
| IS4 mAb/cardiolipin | NA | NA | 12.0 |
| IS6 mAb/cardiolipin | NA | NA | ~1000 |
| 2F5 peptide-lipid, encounter | 510 | 0.15 | |
| 2F5 peptide-lipid, docking | 0.05 ($s^{-1}$) | 3.3 | 1.8 |
| 4E10 peptide-lipid, encounter | 190 | 0.15 | |
| 4E10 peptide-lipid, docking | 0.02 ($s^{-1}$) | 1.5 | 21.5 |

[a] NA: Due to biphasic nature of binding of mAbs to cardiolipin, $K_d$ values from equilibrium-binding analyses are given. NA*: due to the low level of binding, reliable rate constants could not be measured.

For mAb binding to peptide-lipid conjugates, rate constants for the encounter and docking steps were determined by curve fitting to the conformational change model. Mean and SE data are provided for binding studies in which at least three independent studies were performed.

resuspended in 10 μl of diethyl pyrocarbonate-treated $H_2O$. The modified IS6 RNA was then reverse transcribed with Superscript III reverse transcriptase and an oligo dT primer (Invitrogen Life Technologies).

IS6 cDNA (2 μl) was used in a PCR amplification reaction using the 5′ primers provided by the GeneRacer kit and 3′ primers that are universal for IgG genes. GeneRacer 5′ primer: 5′-CGACTGGAGCACGAGGACA CTGA-3′ with 3′ gene specific primers uni-κ: 5′-GAAGATGAAGACA GATGGTGC-3′, uni-λ: 5′-AGTGTCGCCTTGTTGGCTTG-3′ or uni-γ: 5′-GTAGTCCTTGACCAGGCA-3′ were used in the first round PCR amplification. GeneRacer 5′ nested primer: 5′-GGACACTGACATGGACT GAAGGAGTA-3′ and the same 3′ primers were used in the second PCR amplification. The following PCR condition was used for each round of amplification: 30 cycles of denaturation at 94°C for 45 s, annealing at 50°C for 45 s, and extension at 72°C for 2 min.

### *Cloning and sequencing of amplified DNA*

The amplified product products were run on a 1% agarose gel, visualized with ethidium bromide staining, and purified with a gel extraction kit (Qiagen). The purified products were ligated into PST-1 Blue plasmids (Novagen) and sequenced using T7 and SP6 primers.

## Results

### *Reactivity of membrane proximal mAbs 2F5 and 4E10 to cardiolipin and HIV-1 Env epitopes*

To directly compare the binding properties of anti-HIV-1 2F5 and 4E10 membrane proximal mAbs with anti-cardiolipin autoantibodies from APS patients, we have used SPR measurements to calculate the affinity of whole and Fab of 2F5 and 4E10 mAb binding to cardiolipin. The scheme used to measure binding of mAbs to cardiolipin and peptide epitopes is shown in Fig. 1. Both 4E10 (Fig. 1*A*) and 2F5 mAbs (Fig. 1*C*) bound to sensor surfaces with immobilized cardiolipin. The specific binding to cardiolipin was derived by subtraction of nonspecific binding to a BSA immobilized surface. The specificity of membrane proximal mAb binding to the aqueous form of cardiolipin was also confirmed in comparison to two control proteins, BSA and OVA, using a human anti-gp120 CD4 inducible mAb, 17b as an Ab control (30, 31) (data not shown). 4E10 and 2F5 mAbs bound specifically to cardiolipin with $K_D$ values of 37 nM and 0.35 μM, respectively (Fig. 1, *A* and *C*). Moreover, 4E10 bound with fast association kinetics and a biphasic dissociation phase. Nevertheless, both 4E10 and 2F5 mAb showed specific binding to cardiolipin, with a relatively lower $K_d$ value for 4E10 mAb (37 nM) than that for 2F5 mAb (0.35 μM).

High-affinity binding of whole Ab (IgG) is often due to the avidity effect associated with the bivalency of IgG molecule (36, 37). Thus, we have compared the reactivity of 2F5 and 4E10 mAbs vs their Fab to both HIV-1 Env gp41 epitopes and to cardiolipin. As observed with whole IgG, both 4E10 and 2F5 Fabs specifically bound to cardiolipin (Fig. 1, *B* and *D*). However, 4E10 Fab bound to cardiolipin with $K_d$ of 1.2 μM (Fig. 1*B*), which was ~30-fold lower than those measured with 4E10 IgG (37 nM, Fig. 1*A*). Such differences are comparable to those observed with 4E10 and 2F5 IgG vs Fab binding to nominal epitope peptides. 4E10 Fab binding to its nominal epitope peptide was 10-fold weaker ($K_d$ = 19 and 244 nM for 4E10 IgG and Fab, respectively, Fig. 1, *E* and *F*, Table I), while 2F5 Fab binding was 20-fold lower when compared with 2F5 IgG ($K_d$ = 0.3 and 7.5 nM for 2F5 IgG and Fab, respectively, Fig. 1, *G* and *H*, and Table I). In both cases, the lowering in $K_d$ values for Fab was due to faster off-rates (Table I), which is consistent with earlier SPR studies in which binding kinetics of other monovalent and bivalent Ab ligands have been compared (38).

It was noted that 4E10 IgG bound to cardiolipin with biphasic off-rates (Fig. 1*A*), with the slower component being predominant. The binding kinetics of 4E10 Fab to cardiolipin was also similar in being biphasic, but with the faster component being predominant (Fig. 1*B*). The faster off-rates of 4E10 Fab were 2.5 times faster than those observed with whole IgG ($k_d$ (fast) = 0.1 $s^{-1}$ and 0.04 $s^{-1}$ for IgG and Fab, respectively). Because the slower dissociation phase was observed with both 4E10 IgG and Fab, this component was not due to the bivalency of IgG molecule. We have ruled out aggregation or dimerization as a possible explanation, because we confirmed by size exclusion chromatography (Superdex HR200) that there were no aggregates or dimers present in the Fab preparation (data not shown). Furthermore, the faster association phase of 4E10 mAb binding was found to be dependent on the net charge of the polar head groups (data not shown). 4E10 mAb bound to the anionic phospholipid, cardiolipin (net charge = −2), containing liposomes more strongly than those with phosphatidic acid (net charge = −1) or sphingomyelin (net

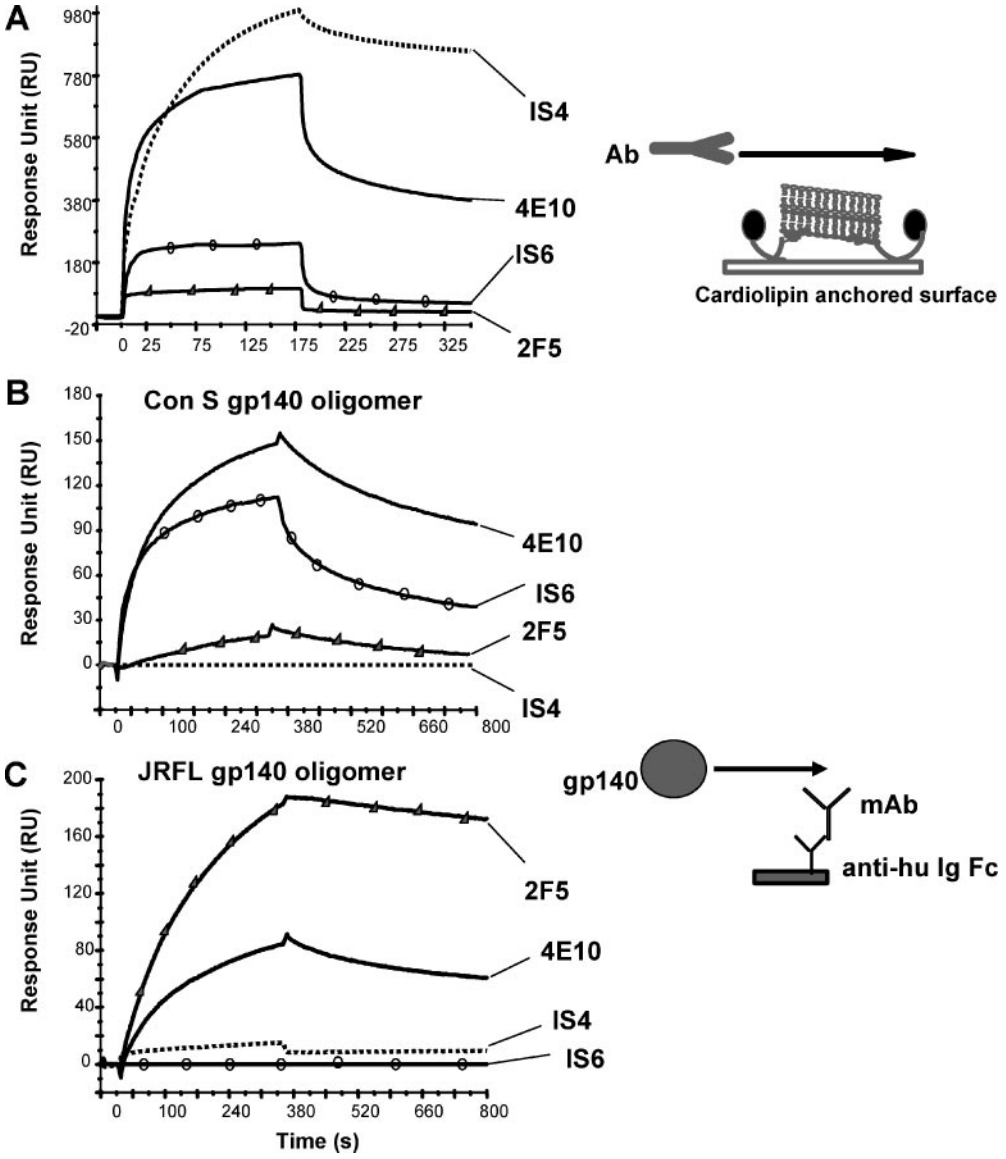


**FIGURE 2.** Interactions of anti-MPER mAb and anti-cardiolipin mAbs to cardiolipin and rHIV-1 Env gp140. *A*, Binding of anti-cardiolipin mAbs (IS4, IS6) and anti-HIV-1 MPER mAbs (2F5, 4E10) to anchored cardiolipin. A total of 100 $\mu$g/ml of each mAb was injected over 500 RU of cardiolipin anchored on a L1 sensor chip. Binding of mAb IS6 to Con S gp140 but not to JRFL gp140. Each of the mAb was captured at ~1,000 RU on a surface immobilized with anti-human Ig Fc (13,000 RU). rEnv gp140, Con S (*B*), or JRFL (*C*), was injected over each surface anchored with either mAb 4E10 (solid line), 2F5 (▲), IS4 (dotted line), or IS6 (●). Binding kinetics data are given in Table I. CDRH3 sequences of each mAb is given and the hydrophobic loop is underlined. 2F5 and 4E10 are from Protein Data Bank code 1TJI and ITZG, respectively. IS6 IgG was sequenced as described in *Materials and Methods* and the sequence for IS4 mAb were from Zhu et al. (29). IS4 GRRDVRGVLWRGRHD; IS6 DRSGRRQRWGMGY; 2F5 RRGPTTLFGVPIARG-PVNAMDV; 4E10 EGTTGWGWLGKPIGAFAH.

charge = 0). However, binding to sphingomyelin containing liposomes show that there is a second component (with slower binding kinetics) of 4E10 mAb interactions which was not related to the charge on the lipid polar head groups. In comparison to the 4E10 Fab, the 2F5 Fab bound with a comparable $K_d$ value to cardiolipin as did 2F5 IgG (Fig. 1, *C* and *D*). However, the binding association rates of 2F5 Fab was much slower and did not reach steady state, even after several minutes of injections. This slow association rate was not due to diffusion limited binding (mass transport limitation) as it could not be overcome either by faster flow rates or lower cardiolipin immobilization density. Overall, the comparison of bivalent IgG to Fab binding confirmed the specificity of 4E10 and 2F5 for cardiolipin and showed that the binding $K_d$ of 4E10 and 2F5 Fabs for cardiolipin is in the low micromolar range.

*Comparison of lipid reactivity of anti-gp41 membrane proximal mAbs with human anti-cardiolipin autoantibodies*

We next compared two anti-cardiolipin autoantibody mAbs (IS4 and IS6), derived from an APS patient, to mAbs 2F5 and 4E10 in direct binding assays to cardiolipin. We could detect two patterns of mAb binding to cardiolipin: one, a relatively strong and a second weak binding profile (Fig. 2*A*). mAb IS4 bound strongly to cardiolipin with nM $K_d$ which was similar to those of mAb 4E10 (Fig. 2*A*, Table I). However, both 2F5 and IS6 bound to cardiolipin weakly with micromolar $K_d$ (Fig. 2*A*, Table I). As observed earlier with 2F5 and 4E10 Fabs, the binding of IS6 Fab to cardiolipin was also biphasic and was associated with faster dissociation rates. Although we have analyzed only two APS mAbs, these data suggested that there is likely a wide range of apparent cardiolipin

binding $K_d$ (nanomoles to micromoles) of anti-cardiolipin autoantibodies and that the cardiolipin binding $K_d$ measured for 2F5 and 4E10 mAbs lie within this range.

IS4 mAb was more promiscuous and showed much less discrimination when binding to phospholipids in liposomal form with varying net polar head group charges (data not shown). However, 4E10 mAb, was more specific for cardiolipin, with strong preference for cardiolipin-containing liposomes (cardiolipin > PC:cardiolipin ≫ phosphatidylcholine:phosphatidylserine; data not shown) and only bound weakly to other phospholipids in liposomes. No such pattern was observed with either IS6 or 2F5 mAbs.

The anti-cardiolipin autoantibody IS4 mAb did not cross-react with any recombinant HIV-1 Env proteins (Fig. 2, *B* and *C*). This was also true for IS6, with one exception. IS6 mAb bound well to the group M consensus CON-S gp140 oligomer with $K_d$ of 407 nM (Fig. 2*B*, Table I). IS6 bound with relatively faster kinetics and about 3-fold lower $K_d$ than mAb 4E10 binding to CON-S gp140 oligomers (Table I).

The binding kinetics of 2F5 mAb for rHIV-1 gp140 Env was dependent on the Env protein used, with 2F5 mAb binding weakly to the group M consensus Env CON-S gp140 and strongly to the wild-type clade B HIV-1 JRFL gp140 (Fig. 2, *B* and *C*). The binding of IS6 mAb to CON-S gp140 could not be blocked with either 2F5 or 4E10 epitope peptides. Furthermore, in a direct binding assay, IS6 mAb did not bind to either of the above peptides when the peptides were anchored on a SA-sensor chip (data not shown). Taken together, these data suggested that IS6 mAb interacted at sites that lie outside the membrane proximal region of gp41 on CON-S gp140 oligomer and demonstrated that anti-cardiolipin mAbs from autoimmune disease patients might cross-react with select HIV-1 Env proteins.

### *CDR3 sequence similarities of gp41 membrane proximal mAbs and anti-cardiolipin mAbs*

We have sequenced IS6 $V_H$ CDR3 and compared CDR H3 sequences of APS mAbs, IS4 (29) and IS6, with 2F5 and 4E10 mAbs (1, 2). These CDR3 sequences highlighted several similarities between the membrane proximal mAbs and the APS mAbs. First, both groups of mAbs have a highly hydrophobic patch in their long CDR3 loop (Fig. 2 legend, CDR3 sequences underlined). This highly hydrophobic domain, termed "the heel" of the CDR3 "feet," minimally interacts with the gp41 epitope peptide and was proposed to interact with as yet unidentified virion component (1, 2). Second, there are several arginine (Arg) residues in both groups of mAbs. Among the anti-cardiolipin mAbs, the position of Arg appears to be critical for binding to cardiolipin and dsDNA (27, 39, 40). Although the preferred positions are surface exposed Arg (between positions 95–100); a negative correlation of Arg at position 95, 97 has also been reported (27, 39). Of the four exposed Arg residues in IS4 $V_H$, those in positions 100 and 100g had a major influence on the strength of cardiolipin binding, while those at 96 and 97 had no effect (26, 27). 2F5 mAb has an Arg at one key position of 100 and also includes them at positions 95, 96. In the case of 4E10 mAb, however, there are no Arg in the CDR3, although CDR1 and CDR2 Arg could influence cardiolipin binding. Thus, these sequence analyses show that there are similarities between the two groups of mAbs, and that a hydrophobic patch in the CDR3 loop could account for mAbs 2F5 and 4E10 binding to anionic phospholipids.

Comparison of the isotypes of all four mAbs revealed that all originally derived Abs were IgG3, suggesting the possible origins of these Abs from B cell compartments in which there is preferential class switching from IgM to IgG3 such as the human equivalents of mouse B1, transitional, and marginal zone B cells (41–43).

### *Interaction of mAbs 2F5 and 4E10 with lipid-associated peptide epitopes (peptide-lipid conjugates)*

A key question relevant to gp41 membrane proximal mAb polyreactivity is the significance of this property of lipid reactivity of 2F5 and 4E10 mAbs in binding to epitope peptide-lipid complexes. The inability of soluble HIV-1 Env with membrane proximal region epitopes to elicit broadly neutralizing Abs and the crystal structures of 2F5 and 4E10 mAbs complexed with their gp41 epitopes highlight the importance of an unidentified virion component that may be lacking in the gp41 membrane proximal sequence when presented either as a peptide or in the form of soluble gp41 (1, 2, 44). Ofek et al. (1) and Grundner et al. (45) found that the binding of 2F5 mAb was enhanced in flow cytometric analysis when HIV-1 gp160 was embedded in proteoliposomes. This suggested that the gp41 membrane proximal region in the lipid-associated bound form presented a unique conformation to which the mAb bound to with higher affinity, or alternatively, that the membrane proximal mAbs directly interacted with a membrane component via its CDR3 loop, resulting in the enhancement of the stability of the mAb-membrane proximal complex.

To address this issue, we prepared synthetic liposomes in which were anchored the 2F5 and 4E10 HIV-1 gp41 nominal epitope peptides using an $\alpha$-helical linker sequence (GTH1-gag Th epitope) which was conjugated N terminus to the gp41 2F5 or 4E10 sequence. As shown in Fig. 3, presentation of peptide epitopes on synthetic liposomes resulted in specific binding of 4E10 and 2F5 mAbs to their respective nominal peptide epitopes. Although low levels of binding of both mAbs to either liposomes with no peptide or to liposomes presenting the irrelevant peptide were detected (Fig. 3, *A* and *B*), the binding of both mAbs to the gp41 peptide liposome conjugate was essentially peptide specific. No binding of the control mAb 17b to any liposomes were detected (Fig. 3*C*). Furthermore, the binding of both mAbs to peptide-liposome conjugates showed remarkably different binding profiles when compared with binding to the nominal gp41 epitopes alone (Fig. 1). Binding of 2F5 and 4E10 mAbs to their respective peptide-liposomes conjugates were biphasic (Fig. 3, *D* and *E*) and could be best defined by a two-step, conformational change model ($A + B \rightarrow ABx$; $ABx \rightarrow AB$). This model has previously been used to describe conformational rearrangements associated with soluble CD4 binding to HIV-1 gp120 (46) and as well for anti-hen egg lysozyme Fabs to describe a linked two-step process involving molecular encounter and docking (47, 48). In this model, the first step is described as an encounter step that results in the formation of the first less stable complex (ABx) with faster kinetics ($k_{a1}$ and $k_{d1}$). The encounter step then leads to a docking step which involves a conformational change resulting in the formation of a more stable complex (AB) with much slower off-rates ($k_{d2}$) (Table I).

To confirm that the binding of 4E10 and 2F5 mAbs to peptide-liposome conjugates indeed followed a sequential two-step model, we first determined whether Fab of 4E10 and 2F5 would also bind in a similar mode. Both 4E10 and 2F5 Fab binding to their respective peptide-lipid conjugates could be described by the two-step conformational change model (Fig. 3, *F* and *G*). Next, we measured the initial off-rates of mAb binding to peptide-liposomes at varying contact times. An inverse relationship was observed between off-rate and the association time (Ta), which suggested that the two phases of the binding interactions were linked, and that the events occurred in a sequential manner (Fig. 4). It is of

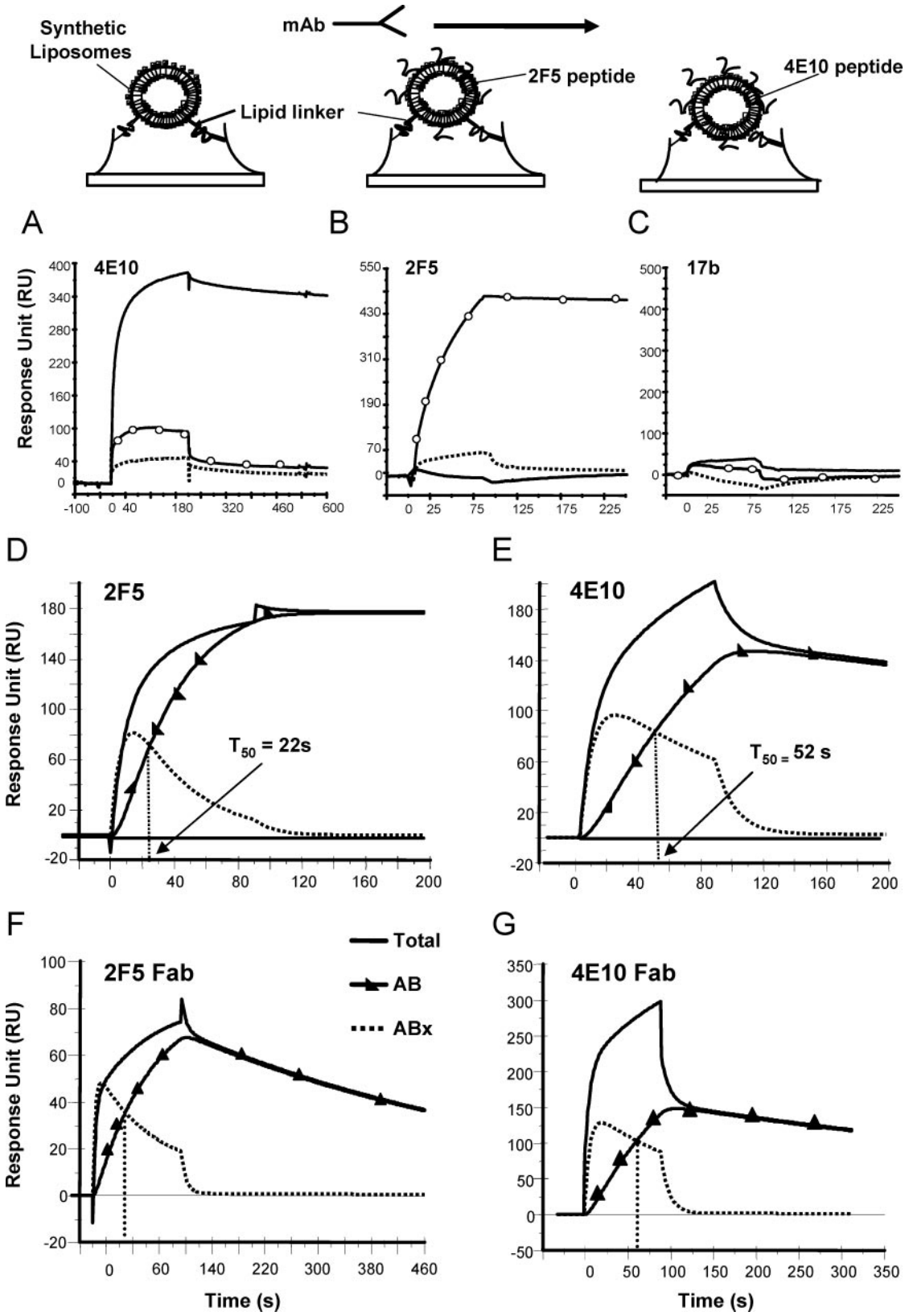


**FIGURE 3.** mAbs 4E10 and 2F5 binding to peptide-liposome conjugates. Approximately 600 RU of either synthetic liposomes (broken line); 2F5 peptide-liposomes (○); or 4E10 peptide-liposomes were coupled on to a BIAcore L1 sensor chip. mAbs 4E10 (*A*), 2F5 (*B*), or 17b (*C*) was then injected at 100 $\mu$g/ml. Both 4E10 and 2F5 bound to peptide-liposomes in a peptide-dependent manner. *D–G*, The binding of mAbs or Fab of 4E10 and 2F5 to their respective epitope peptide-liposome conjugates follows the two-step conformational change model. Curve-fitting analysis of data generated from binding of mAb 4E10 and 2F5 to their respective peptide-liposome conjugates. The two-step conformational change model was used to derive the rate constants for the encounter complex (●) and the docked complex (▲) and is given in Table I. In each of the overlay, the binding data is shown in solid line and represents the observed total binding response. The component curves for the encounter complex (●) and the docked complex (▲) were simulated from the experimentally determined rate constants. $T_{50}$ defines the time required for half of the encounter complex to be converted to docked complex. Both mAbs bound to their peptide-liposomes with an overall high apparent $K_d$ (Table I).

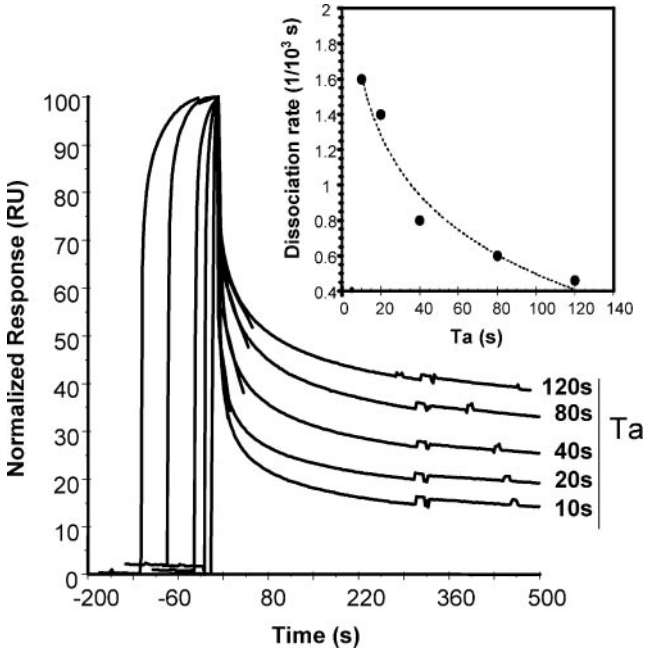


**FIGURE 4.** Effect of varying contact time on dissociation rates. 4E10 mAb (100 $\mu$g/ml) was injected with varying contact time (Ta) in seconds (10, 20, 40, 80, and 120) over 600 RU of 4E10 peptide-liposomes immobilized surface. Binding data were normalized to 100 RU and the end of injection point (start of dissociation) was aligned on the *x*-axis at time zero. Dissociation rate constants were measured during the first 60 s of the dissociation phase and were plotted against Ta (*inset*). An inverse relationship between early dissociation rates and Ta shows that the two steps (encounter and docking) of the binding of the mAb are linked and sequential.

interest to note that the $T_{50}$, where the component curves crossed and defined the amount of time required for half of the encounter complexes to be converted to docked complexes, of 2F5 mAb or Fab binding was 2-fold lower than that of 4E10 mAb or Fab binding (Fig. 3). These data suggested a more favorable complex formation for 2F5 mAb, possibly due to differences in peptide conformers on the liposome surface. Overall, these data suggested that the phospholipid binding property of neutralizing mAbs might be exploited by the mAb for initially gaining proximity or aligning of the Ag-binding sites of the mAbs, and thereby leading to a more stable and specific interaction with gp41 peptide.

### *Temperature-dependent binding of 4E10 and 2F5 mAb binding to a peptide-liposome complex*

To define the mechanism of the binding of the membrane proximal mAbs to peptide-liposome conjugates, we have measured the effect of temperature on the binding of 4E10 and 2F5 mAbs to peptide-liposome conjugates. Binding of 4E10 and 2F5 mAbs to their respective peptide-liposomes and their epitope peptides were measured at temperatures ranging from 5 to 30°C. We found binding of 2F5 mAb to 2F5 nominal epitope peptide was relatively stable over the temperatures range studied (Fig. 5*A*), while 4E10 mAb binding showed moderate effects with faster single-phase kinetics at higher temperatures (Fig. 5*C*). In contrast, the effect of temperature on mAb binding to peptide liposome conjugates was strikingly different. The docking step of both 4E10 and 2F5 mAb was rate limiting, because increasing temperature had an adverse effect on the docking step but not on the encounter step, with both mAbs forming less stable complexes at higher temperatures (Fig. 5, *B* and *D*). The free energy change ($\Delta$G) of the interactions remained the same over the entire temperature range (Table II). Although the contribution of the encounter step ($\Delta$G1) was ~8–9 kcal, there was no effect of temperature on this step. In contrast, docking of the mAbs to the liposomes, that contributed ~25% of the total $\Delta$G at 5°C, was reduced to 12 and 15% for 4E10 and 2F5 mAb, at 30°C, respectively. Increasing temperatures had an adverse effect on both the forward ($k_{a2}$) and backward ($k_{d2}$) rate constants of the docking step of the mAb reactions. Although $k_{a2}$ rates became progressively slower, $k_{d2}$ rates became faster with increasing temperature. These data indicated that with each increase in temperature, smaller fractions of the encounter complex would be able to form a stable docking complex. These observations implied that

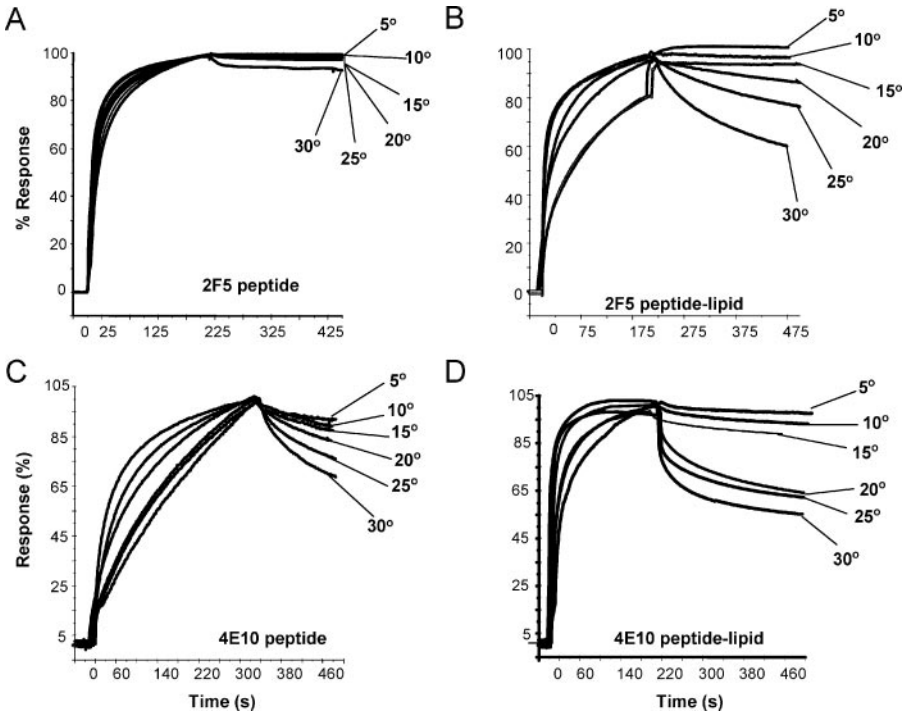


**FIGURE 5.** Effect of temperature on binding kinetics of 2F5 and 4E10 mAb to peptide and peptide-lipid conjugates. Binding kinetics of 2F5 (*A* and *B*) and 4E10 (*C* and *D*) was measured at temperatures ranging from 5 to 30°C for their respective epitope peptide (*A* and *C*) or peptide-lipid conjugate (*B* and *D*). Specific binding signal was recorded in reference to either control peptide or synthetic liposomes as described in *Materials and Methods*. Data shown are expressed as the percent response and was derived following normalization of binding responses recorded at each temperature.

Table II. *Effect of temperature on binding parameters of 2F5 and 4E10 mAb complexes with peptide-liposome conjugates*

| Parameter | 4E10 | | | 2F5 | | |
|---|---|---|---|---|---|---|
| | 5ºC | 20ºC | 30ºC | 5ºC | 20ºC | 30ºC |
| Rate constants | | | | | | |
| $k_a1$ ($10^5$ $M^{-1}$ $s^{-1}$) | 0.55 | 1.40 | 1.26 | 2.1 | 1.0 | 0.97 |
| $k_d1$ ($10^{-2}$ $s^{-1}$) | 1.93 | 1.62 | 1.77 | 5.7 | 4.1 | 3.7 |
| $k_a2$ ($10^{-2}$ $s^{-1}$) | 1.43 | 0.64 | 0.57 | 2.3 | 1.3 | 1.4 |
| $k_d2$ ($10^{-4}$ $s^{-1}$) | 1.1 | 5.6 | 6.5 | 0.8 | 2.6 | 9.3 |
| Binding constants | | | | | | |
| $K_d$ ($10^{-8}$ M) | 0.3 | 0.6 | 1.4 | 0.1 | 0.4 | 4.2 |
| $K_d1$ ($10^{-7}$ M) | 3.5 | 1.2 | 1.4 | 2.7 | 4.1 | 3.8 |
| $K_d2$ ($10^{-2}$) | 0.8 | 8.8 | 11.5 | 0.35 | 2.0 | 6.6 |
| Free energy changes | | | | | | |
| ΔG (kcal) | −10.9 | −10.8 | −10.9 | −11.5 | −11.0 | −10.2 |
| ΔG1 (kcal) | −8.2 | −9.3 | −9.5 | −8.4 | −8.6 | −8.9 |
| ΔG2 (kcal) | −2.7 | −1.4 | −1.3 | −3.1 | −2.3 | −1.5 |
| %ΔG (ΔG2/ΔG) | 25% | 13% | 12% | 27% | 21% | 15% |

the first step of the interaction (encounter) was thermodynamically more favorable, while the docking step involved an induced-fit process suggestive of an entropic/conformational barrier. The presence of the lipid in these peptide-liposome conjugates likely imposed a constraint on the peptide conformation making it out less favorable for stable docking of the mAbs.

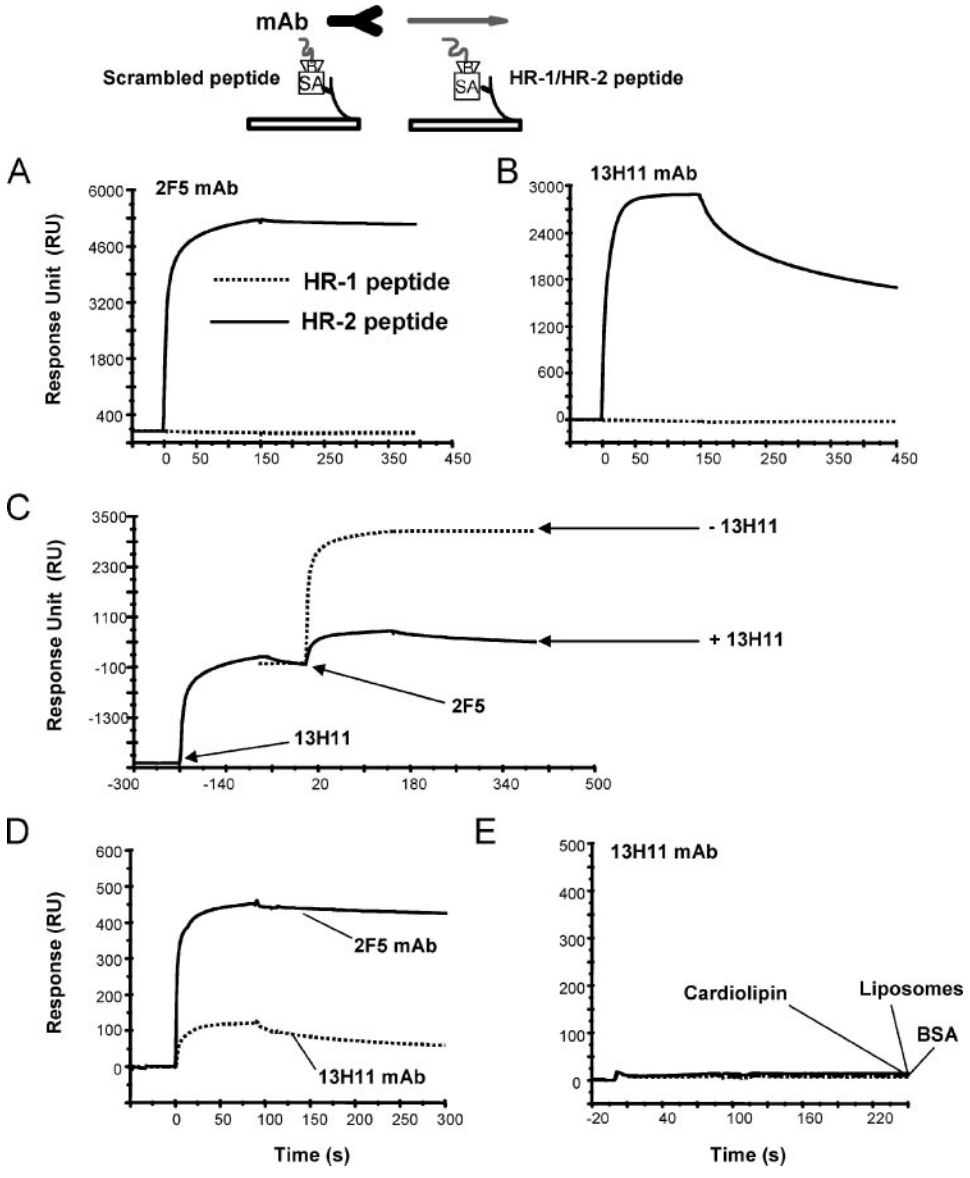


**FIGURE 6.** Binding of a non-neutralizing mAb, 13H11, to MPER peptides. *A* and *B*, Binding of MPER mAb 2F5 (*A*), 13H11 mAb (*B*) to the full-length HR-2 peptide (YTSLIHSL IEESQNQQEKNEQELLELDKWAS LWNF; solid line), and to the control HR-1 peptide (dotted line). *C*, Blocking of 2F5 mAb binding to the full-length HR-2 peptide, DP178, by 13H11 mAb. 13H11 mAb was bound to saturation and then mAb 2F5 was injected at the time indicated with arrows. The binding of mAb 25F in the absence (dotted line) or presence (solid line) of prebound 13H11 is shown. *D*, Comparison of 13H11 mAb (dotted line) to 2F5 mAb binding to 2F5 peptide-lipid conjugates. *E*, Binding of 13H11 mAb (100 μg/ml) to cardiolipin, synthetic liposomes, or BSA-immobilized surfaces.

Table III. *Binding reactivity of anti-HIV-1 MPER mAbs and anti-cardiolipin mAbs*[a]

| mAb | 2F5 | 4E10 | 13H11 | IS4 | IS6 |
|---|---|---|---|---|---|
| Cardiolipin | + | ++ | − | ++ | + |
| Liposomes | +/− | +/− | − | +/− | +/− |
| Env gp140 (Con-S) | + | ++ | + | − | + |
| MPER peptide epitope | ++ | ++ | ++ | − | − |
| MPER peptide lipid | ++ | ++ | +/− | +/− | − |

[a] +++, Strong binding with $K_d < 100$ nM; +, weak binding with $K_d > 100$ nM–$\mu$M; −, no binding; +/−, very low-affinity binding with extremely fast kinetics. Synthetic liposomes were of the following composition, POPC:POPE:DMPA:Chol, and as described in *Materials and Methods*.

### *Binding properties of a non-neutralizing anti-HIV-1 membrane proximal mAb*

If polyreactivity and lipid binding and the two-step conformational change associated binding of 2F5 and 4E10 mAbs to peptide-liposome conjugates are associated with mAb ability to neutralize HIV-1, then it is likely that these properties would be lacking in a non-neutralizing gp41 membrane proximal region-reactive mAb. Thus, we have characterized the binding properties of a novel anti-gp41 membrane proximal mAb 13H11, which was raised in mice immunized with HIV-1 gp140 Env oligomer that expressed the 2F5 epitope. 13H11 mAb was similar to 2F5 mAb and bound to the gp41 heptad repeat-2 (HR-2) peptide, DP178, and not to the gp41 HR-1 peptide, DP107 (Fig. 6, *A* and *B*). 13H11 bound to the full-length HR-2 peptide (DP178) with nanomolar affinity (Table I). Interestingly, 13H11 and 2F5 mAb could cross-block their binding to DP178 (Fig. 6*C*). Unlike 2F5 mAb, however, 13H11 mAb did not bind to any phospholipid, including cardiolipin (Fig. 6*E*). Furthermore, 13H11 binding to 2F5 peptide-liposome conjugates was minimal and showed low-level binding with a fast association and a dissociation rate, which was about a log faster when compared with 2F5 mAb (Fig. 6*D*). Finally, an additional distinguishing feature of 13H11 mAb was that, unlike mAb 2F5, it did not neutralize any of four HIV-1 primary isolates tested (data not shown).

Overall, the comparison of the three groups of mAbs: anti-cardiolipin (IS4, IS6), neutralizing anti-HIV-1 MPER (2F5, 4E10), and non-neutralizing anti-HIV-1 MPER (13H11) highlights several key features (Table III) that are relevant to understanding the properties of anti-HIV-1 MPER-neutralizing mAbs. First, neutralizing mAbs show cross-reactivity with phospholipids (weak), which include cardiolipin (strong). Second, both neutralizing mAbs were able to bind strongly to peptide epitopes presented on synthetic liposomes. This appears to be an important distinction when 2F5 and 4E10 mAbs are compared with the non-neutralizing mAb 13H11, which showed no reactivity to phospholipids and bound weakly to MPER peptide presented on liposomes (Table III).

## Discussion

SPR assays were used to characterize both 2F5 and 4E10 anti-HIV-1 Env Abs and anti-cardiolipin mAbs from an autoimmune disease patient to a spectrum of lipid-containing Ags. We found that both 2F5 and 4E10 membrane proximal anti-Env mAbs bound to cardiolipin in affinities that were similar to anti-cardiolipin autoantibodies derived from autoimmune disease patients, providing additional support for the notion that 2F5 and 4E10 are autoantibodies. We also found that the binding of 2F5 and 4E10 mAbs to epitope peptide-liposome conjugates is described by an induced fit conformational change model. The induction of conformational rearrangements that lead to stable docking of membrane proximal mAb to peptide-liposome conjugates was temperature dependent, being unfavorable at higher temperatures. Finally, we have produced a nonpolyreactive mAb that cross-blocks the binding of mAb 2F5, yet is non-neutralizing.

Using ELISA, we had earlier reported that mAbs 4E10 and 2F5 bound to cardiolipin with nanomolar and micromolar affinity, respectively (15). Compared with ELISA, an advantage of SPR-binding assays is that they allow capture of cardiolipin and other phospholipids in aqueous suspensions via an alkyl linker on a BIAcore L1 sensor chips. Using both whole mAbs and their Fab, we have demonstrated that the binding $K_d$ of anti-gp41 membrane proximal mAbs for cardiolipin is similar to those of anti-cardiolipin mAbs for cardiolipin. The avidity effect and the change from nanomoles to micromoles in 4E10 binding $K_d$ as seen when comparing whole Ab with Fab was expected and has been reported for other anti-lipid autoantibodies (49). Analysis of the two anti-cardiolipin autoantibodies also revealed structural similarities with the anti-HIV-1 membrane proximal mAbs, with each mAb having long CDR3 regions and similarly placed arginine residues. Because neither of the two anti-cardiolipin mAbs derived from an APS patient had anti-HIV-1-neutralizing activity, the ability of an Ab from a HIV-1-negative patient to bind to cardiolipin per se does not guarantee the ability to neutralize HIV-1. It is also important to note that anti-cardiolipin activity of 2F5 and 4E10 is not necessarily related to Ab pathogenicity in autoimmune diseases like APS (21, 22, 50).

Rather, reactivity of anti-cardiolipin Abs with the first domain of $\beta$-2-glycoprotein-1 is more predictive of pathogenicity (24, 25). We found that the mAbs 2F5 and IS6 binding to cardiolipin was enhanced by $\beta$-2-glycoprotein-1 while IS4 and 4E10 binding were not (M. Alam, B. Haynes, unpublished observations). 2F5 and 4E10 mAb reactivity has been administered to a number of HIV-1-infected patients with no thrombotic event noted (51), although when these mAbs are administered, patient sera become positive in anti-cardiolipin and lupus anti-coagulant Ab assays (52). However, the MPER mAbs, 2F5 and 4E10, were not the contributing factor in the minimal effect observed on viral load (51, 53). Thus, while these Abs may not be pathogenic and not cause thrombotic disease when administered to $HIV^+$ patients, the relevance of our study resides in the notion that 2F5 and 4E10 have polyreactivity for various self Ags, and have structural and reactivity pattern similarities to known autoantibodies. These observations support the hypothesis that 2F5 and 4E10-like Abs are controlled by negative immunoregulatory mechanisms.

The significance of polyspecific lipid reactivity of anti-HIV-1 gp41 membrane proximal mAbs may lie in their ability to interact with membrane proximal peptide epitopes in concert with the viral lipid membrane. Evidence in support of this notion comes from the observation of Ofek et al. and Cardoso et al. (1, 2) that much of the 2F5 and 4E10 CDR3 regions are available to associate with the virion lipid bilayer. Zhu et al. (54) has recently used electron microscopy tomography to derive a structure of the native Env trimer that when modeled with the crystal structures of 2F5 and 4E10 Fabs suggest both mAb CDR3s can interact with the viral membrane. Additional evidence that mAb lipid polyreactivity is required for 2F5 neutralization of HIV-1 comes from our studies that the anti-membrane proximal mAb 13H11, that cross-blocks the binding of mAb 2F5 to gp41 epitopes, was not cross-reactive with phospholipids and was unable to neutralize HIV-1.

An important finding of our studies is that both mAbs 2F5 and 4E10 are sensitive to conformational changes induced upon anchoring of nominal peptide epitopes into synthetic lipid bilayer. We have observed a difference in the binding mode of both MPER

mAbs when binding to peptide in solution vs peptide conjugated to lipids. The energetics of MPER mAb binding to peptide in solution is thermodynamically favored (temperature sensitive) while being unfavorable to peptides conjugated to lipids (temperature dependent). Because our binding kinetics data fit well to a conformational change model, it may be inferred that the favored lipid-bound conformer of the peptide is induced only upon mAb encounter and following conformational rearrangements. However, it is important to note that our observations regarding the temperature dependency of anti-MPER mAbs 2F5 and 4E10 binding is based on artificial lipid-conjugates that were designed using nominal epitope peptides conjugated to a helical linker peptide. These specific peptide-lipid constructs may not be the prefect mimic of the native conformation on the viral membrane surface. Furthermore, the influence of flanking residues of the MPER region and the degree of conformational constraints imposed upon lipid conjugation may be sequence or linker specific.

A key issue is also in determining which part of the 2F5 and 4E10 CDR3 regions binds to the viral membrane and to cardiolipin. As mentioned, structural studies strongly suggest that the hydrophobic patches of 2F5 and 4E10 CDR3 will interact with the viral membrane (1, 2, 54). In contrast, we demonstrated that an antiidiotypic Ab against the 2F5 CDR3 gp41-binding site blocked the binding of 2F5 to cardiolipin (15). Moreover, Sanchez-Martinez et al. (55) have demonstrated that cardiolipin liposomes could inhibit the neutralizing activity of mAb 2F5. Thus, 2F5 mAb might have two distinct lipid-binding sites: the gp41-binding site that cross-reacts with cardiolipin, and the hydrophobic portion of the CDR3 region that likely interacts with the viral membrane.

An additional problem in HIV-1 vaccine development is the difficulty to design an immunogen that is a mimic of the 4E10 or 2F5 epitope in the native HIV-1 trimer. The bound state of 2F5 epitope is in a more open conformation (1), while the 4E10 epitope is not completely $\alpha$-helical (2). Thus, approaches that either introduces conformational constraints that lead to improved complementarity/affinity of mAb binding (56) or mimic membrane-bound conformations, as described in this study, might provide more useful immunogens. Alternative designs of peptide-lipid conjugates and a better understanding of the conformation of epitope peptides when anchored into liposomes, would therefore, be useful in designing novel immunogens for the generation of neutralizing anti-MPER mAbs. Finally, our data showing that 2F5 and 4E10 mAbs share many binding and structural similarities to anti-cardiolipin autoantibodies from HIV-1-negative patients suggests that induction of 2F5 and 4E10-like Abs by vaccines or natural infection may be limited by immune tolerance mechanisms (15, 16). Studies are underway to determine the B cells of origin of 2F5 and 4E10-like Abs and to determine their immunoregulatory control.

## Acknowledgments

We acknowledge the gifts of 4E10 Fab reagents from Dennis Burton, Ian Wilson, and Rosa Cardosa and 2F5 Fab reagents from Peter Kwong, Gilead Ofek, and Richard Wyatt. We thank Hua-Xin Liao and Shi-Mao Xia for neutralizing assays and acknowledge the expert technical assistance of Kim R. McClammy.

## Disclosures

The authors have no financial conflict of interest.

## References

1. Ofek, G., M. Tang, A. Sambor, H. Katinger, J. R. Mascola, R. Wyatt, and P. D. Kwong. 2004. Structure and mechanistic analysis of the anti-human immunodeficiency virus type 1 antibody 2F5 in complex with its gp41 epitope. *J. Virol.* 78: 10724–10737.
2. Cardoso, R. M., M. B. Zwick, R. L. Stanfield, R. Kunert, J. M. Binley, H. Katinger, D. R. Burton, and I. A. Wilson. 2005. Broadly neutralizing anti-HIV antibody 4E10 recognizes a helical conformation of a highly conserved fusion-associated motif in gp41. *Immunity* 22: 163–173.
3. Stiegler, G., R. Kunert, M. Purtscher, S. Wolbank, R. Voglauer, F. Steindl, and H. Katinger. 2001. A potent cross-clade neutralizing human monoclonal antibody against a novel epitope on gp41 of human immunodeficiency virus type 1. *AIDS Res. Hum. Retroviruses* 17: 1757–1765.
4. D'Souza, M. P., D. Livnat, J. A. Bradac, and S. H. Bridges. 1997. Evaluation of monoclonal antibodies to human immunodeficiency virus type 1 primary isolates by neutralization assays: performance criteria for selecting candidate antibodies for clinical trials. AIDS Clinical Trials Group Antibody Selection Working Group. *J. Infect. Dis.* 175: 1056–1062.
5. Barbato, G. E., P. Baianchi, P. Inagallinella, W. H. Hurni, M. D. Miller, R. Ciliberto, R. Cortrese, R. Bazzo, J. W. Shiver, and A. Pessi. 2003. Structural analysis of the epitope of the anti-HIV antibody 2F5 sheds light into its mechanism of neutralization and HIV fusion. *J. Mol. Biol.* 330: 1101–1115.
6. Muster, T., F. Steindl, M. Purtscher, A. Trkola, A. Klima, G. Himmler, F. Ruker, and H. Katinger. 1993. A conserved neutralizing epitope on gp41 of human immunodeficiency virus type 1. *J. Virol.* 67: 6642–6647.
7. Zwick, M. B., M. Wang, P. Poignard, G. Steigler, H. Katinger, D. R. Burton, and P. W. Parren. 2001. Neutralization synergy of human immunodeficiency virus type 1 primary isolates by cocktails of broadly neutralizing antibodies. *J. Virol.* 75: 12198–12208.
8. Zwick, M. B., R. Jensen, S. Church, W. M. G. Stiegler, R. Kunert, H. Katinger, and D. R. Burton. 2005. Anti-human immunodeficiency virus type 1 (HIV-1) antibodies 2F5 and 4E10 require surprisingly few crucial residues in the membrane-proximal external region of glycoprotein gp41 to neutralize HIV-1. *J. Virol.* 79: 1252–1261.
9. Bures, R., Z. Gaitan, C. Graziosi, K. McGrath, J. Tartaglia, P. Caudrelier, R. El Habib, M. Klein, A. Lazzarin, D. Stablein, et al. 2000. Immunization with recombinant canarypox vectors expressing membrane-anchored glycoprotein 120 followed by glycoprotein 160 boosting fails to generate antibodies that neutralize R5 primary isolates of human immunodeficiency virus type 1. *AIDS Res. Hum. Retroviruses* 16: 2019–2035.
10. Gao, F., E. Weaver, Z. Lu, Y. Li, H.-X. Liao, B. Ma, S. M. Alam, R. Scearce, L. Sutherland, J. Yu, J. Decker, G. Shaw, D. Montefiori, B. Korber, B. Hahn, and B. F. Haynes. 2005. Antigenicity and immunogenicity of a synthetic human immunodeficiency virus type 1 group m consensus envelope glycoprotein. *J. Virol.* 79: 1154–1163.
11. Meffre, E., R. Casellas, and M. Nussenzweig. 2000. Antibody regulation of B cell development. *Nat. Immunol.* 1: 379–385.
12. Meffre, E., M. Milili, C. Blanco-Betancourt, H. Antunes, M. C. Nussenzweig, and C. Schiff. 2001. Immunoglobulin heavy chain expression shapes the B cell receptor repertoire in human B cell development. *J. Clin. Invest.* 108: 879–886.
13. Raaphorst, F., C. Raman, J. Tami, M. Fischbach, and I. Sanz. 1997. Human Ig heavy chain CDR3 regions in adult bone marrow pre-B cells display an adult phenotype of diversity: evidence for structural selection of $D_H$ amino acid sequences. *Int. Immunol.* 9: 1503–1515.
14. Schroeder, H. W., Jr., and P. M. Kirkham. 2000. Marriage, divorce, and promiscuity in human B cells. *Nat. Immunol.* 1: 187–188.
15. Haynes, B. F., J. Fleming, E. W. St. Clair, H. Katinger, G. Stiegler, R. Kunert, J. Robinson, R. M. Scearce, K. Plonk, H. F. Staats, et al. 2005. Cardiolipin polyspecific autoreactivity in two broadly neutralizing HIV-1 antibodies. *Science* 308: 1906–1908.
16. Haynes, B. F., M. A. Moody, L. Verkoczy, G. Kelsoe, and S. M. Alam. 2005. Antibody polyspecificity and neutralization of HIV-1: a hypothesis. *Hum. Antibodies* 14: 59–67.
17. Nemazee, D. A., and K. Burki. 1989. Clonal deletion of B lymphocytes in a transgenic mouse bearing anti-MHC class I antibody genes. *Nature* 337: 562–566.
18. Tiegs, S. L., D. M. Russel, and D. Nemazee. 1993. Receptor editing in self-reactive bone marrow B cells. *J. Exp. Med.* 177: 1009–1020.
19. Gay, D., T. Saunders, S. Camper, and M. Weigert. 1993. Receptor editing: an approach by autoreactive B cells to escape tolerance. *J. Exp. Med.* 177: 999–1008.
20. Wardemann, H., S. Yurasov, A. Schaefer, J. W. Young, E. Meffre, and M. C. Nussenzweig. 2003. Predominant autoantibody production by early human B cell precursors. *Science* 301: 1374–1377.
21. Gharavi, A. E., W. Wilson, and S. Pierangeli. 2003. The molecular basis of antiphospholipid syndrome. *Lupus* 12: 579–583.
22. Hughes, G. R., N. N. Harris, and A. E. Gharavi. 1986. The anticardiolipin syndrome. *J. Rheumatol.* 13: 486–489.
23. Hunt, J. E., H. P. McNeil, G. J. Morgan, R. M. Crameri, and S. A. Krilis. 1992. A phospholipid-$\beta$2-glycoprotein I complex is an antigen for anticardiolipin antibodies occurring in autoimmune disease but not with infection. *Lupus* 1: 75–81.
24. McNally, T., I. J. Mackie, S. J. Machin, and D. A. Isenberg. 1995. Increased levels of $\beta$2 glycoprotein-I antigen and $\beta$2 glycoprotein-I binding antibodies are associated with a history of thromboembolic complications in patients with SLE and primary antiphospholipid syndrome. *Br. J. Rheumatol.* 34: 1031–1036.
25. Tsutsumi, A., E. Matsuura, K. Ichikawa, A. Fujisaka, M. Mukai, S. Kobayashi, and T. Koike. 1996. Antibodies to $\beta$2-glycoprotein I and clinical manifestations in patients with systemic lupus erythematosus. *Arthritis Rheum.* 39: 1466–1474.
26. Giles, I., J. D. Haley, I. S. Nagl, D. A. Isenberg, D. Latchman, and A. Rahman. 2003. Systematic analysis of sequences of human antiphospholipid and anti-$\beta$2-glycoprotein 1 antibodies: the importance of somatic mutations and certain sequence motifs. *Semin. Arthritis Rheum.* 32: 246–265.

27. Giles, I., N. Lambrianides, D. Latchman, P. Chen, R. Chukwuocha, D. Isenberg, and A. Rahman. 2005. The critical role of arginine residues in the binding of human monoclonal antibodies to cardiolipin. *Arthritis Res. Ther.* 7: R47–R56.
28. Chukwuocha, R. 2002. Molecular and genetic characterization of five pathogenic and two non-pathogenic monoclonal antiphospholipid antibodies. *Mol. Immunol.* 39: 299–311.
29. Zhu, M., T. Olee, D. T. Le, R. A. Roubey, B. H. Hahn, V. L. Woods, Jr., and P. P. Chen. 1999. Characterization of IgG monoclonal anti-cardiolipin/anti-$\beta$2GP1 antibodies from two patients with antiphospholipid syndrome reveals three species of antibodies. *Br. J. Haematol.* 105: 102–109.
30. Wyatt, R., J. Moore, M. Accola, E. Desjardin, J. Robinson, and J. Sodroski. 1995. Involvement of the V1/V2 variable loop structure in the exposure of human immunodeficiency virus type 1 gp120 epitopes induced by receptor binding. *J. Virol.* 69: 5723–5733.
31. Wyatt, R., P. D. Kwong, E. Desjardins, R. W. Sweet, J. Robinson, W. A. Hendrickson, and J. Sodroski. 1998. The antigenic structure of the HIV gp120 envelope glycoprotein. *Nature* 393: 705–711.
32. Liao, H.-X., L. Sutherland, S.-M. Xia, M. Brock, R. Scearce, S. Vanleeuwen, S. M. Alam, M. McAdams, E. Weaver, Z. T. Camacho, et al. 2006. A group M consensus envelope glycoprotein induces antibodies that neutralize subsets of subtype B and C HIV-1 primary viruses. *Virology* 353: 268–282.
33. Scearce, R. M., and G. S. Eisenbarth. 1983. Production of monoclonal antibodies reacting with the cytoplasm and surface of differentiated cells. *Methods Enzymol.* 103: 459–469.
34. Earl, P. L., C. C. Broder, D. Long, S. A. Lee, J. Peterson, S. Chakrabarrti, R. W. Doms, and B. Moss. 1994. Native oligomeric human immunodeficiency virus type I envelope glycoproteins elicits diverse monoclonal antibody reactivities. *J. Virol.* 68: 3015–3026.
35. Alam, S. M., C. A. Paleos, H.-X. Liao, R. Scearce, R. Robinson, and B. F. Haynes. 2004. An inducible HIV type I gp41 HR-2 peptide-binding site on HIV type I envelope gp120. *AIDS Res. Hum. Retroviruses* 20: 836–845.
36. Janeway, C. A., P. Travers, M. Walport, and M. Schlomchik. 2005. The recognition of antigen. In *Immunobiology: The Immune System in Health and Disease,* 6th Ed. Garland Science, Taylor and Francis Group, New York and London, pp. 103–130.
37. Ways, J. P., and P. Parham. 1983. The binding of monoclonal antibodies to cell-surface molecules. *Biochem. J.* 216: 423–432.
38. MacKenzie, C. R., T. Hirama, S. Deng, D. Bundle, S. Narang, and N. M. Young. 1996. Analysis by surface plasmon resonance of the influence of valence on the ligand binding affinity and kinetics of an anti-carbohydrate antibody. *J. Biol. Chem.* 271: 1527–1533.
39. Rahman, A. 2004. Autoantibodies, lupus and the science of sabotage. *Rheumatology* 43: 1326–1336.
40. Krishnan, M. R., N. T. Jou, and T. N. Marion. 1996. Correlation between the amino acid position of arginine in $V_H$-CDR3 and specificity for native DNA among autoimmune antibodies. *J. Immunol.* 157: 2430–2439.
41. Klasse, P. J., and J. Blomberg. 1987. Patterns of antibodies to human immunodeficiency virus proteins in different subclasses of IgG. *J. Infect. Dis.* 156: 1026–1030.
42. Loder, F., B. Mutschler, R. J. Ray, C. J. Paige, P. Sideras, R. Torres, M. C. Lamers, and R. Carsetti. 1999. B cell development in the spleen takes place in discrete steps and is determined by the quality of B cell receptor-derived signals. *J. Exp. Med.* 190: 75–89.
43. Sims, G. P., R. Ettinger, Y. Shirota, C. H. Yarboro, G. G. Illei, and P. E. Lipsky. 2005. Identification and characterization of circulating human transitional B cells. *Blood* 105: 4390–4398.
44. McCaughey, G. B., M. Citron, R. Danzeisen, R. Freidinger, V. M. Garsky, W. M. Hurni, J. Joyce, X. Liang, M. Miller, M. Shiver, and M. J. Bogusky. 2003. HIV-1 vaccine development: constrained peptide immunogens show improved binding to the anti-HIV-1 gp41 mAb. *Biochemistry* 42: 3214–3223.
45. Grundner, C., T. Mirazabekov, J. Sodroski, and R. Wyatt. 2002. Solid-phase proteoliposomes containing human immunodeficiency virus envelope glycoproteins. *J. Virol.* 76: 3511–3521.
46. Zhang, W., A. P. Godillot, R. Wyatt, J. Sodroski, and I. Chaiken. 2001. Antibody 17b binding at the coreceptor site weakens the kinetics of the interaction of envelope glycoprotein gp120 with CD4. *Biochemistry* 40: 1662–1670.
47. Lipschultz, C. A., Y. Li, and S. J. Smith-Gill. 2000. Experimental design for analysis of complex kinetics using surface plasmon resonance. *Methods* 20: 310–318.
48. Lipschultz, C. A., A. Yee, S. Mohan, Y. Li, and S. J. Smith-Gill. 2002. Temperature differentially affects encounter and docking thermodynamics of antibody–antigen association. *J. Mol. Recog.* 15: 44–52.
49. Boffey, J., D. Nicholl, E. R. Wagner, K. Townson, C. Goodyear, K. Furkawa, J. Conner, and H. J. Willison. 2004. Innate murine B cells produce anti-disialosyl antibodies reactive with *Campylobacter jejuni* LPS and gangliosides that are polyreactive and encoded by a restricted set of unmutated V genes. *J. Neuroimmunol.* 152: 98–111.
50. Vila, P., M. C. Hernandez, M. F. Lopez-Fernandez, and J. Batlle. 1994. Prevalence, follow-up and clinical significance of the anticardiolipin antibodies in normal subjects. *Thromb. Haemost.* 72: 209–213.
51. Trkola, A., H. Kuster, P. Rusert, B. Joos, M. Fischer, C. Leemann, A. Manrique, M. Huber, M. Rehr, A. Oxenius, et al. 2005. Delay of HIV-1 rebound after cessation of antiretroviral therapy through passive transfer of human neutralizing antibodies. *Nat. Med.* 11: 615–622.
52. Markowitz, M. 2006. Monoclonal antibody infusions delay HIV-1 rebound after discontinuation of ARV therapy. In *13th Conference on Retroviruses and Opportunistic Infections 2006, February 5–8*, Denver, CO, Abstract 178.
53. Joos, B., A. Trkola, H. Kuster, L. Aceto, M. Fischer, G. Steigler, C. Ambruster, B. Vcelar, H. Katinger, and H. F. Gunthard. 2006. Long-term multiple-dose pharmacokinetics of human monoclonal antibodies (mAbs) against human immunodeficiency virus type 1 envelope gp120 (mAb 2G12) and gp41 (mAbs 4E10 and 2F5). *Antimicrob. Agents Chemother.* 50: 1773–1779.
54. Zhu, P., J. Liu, J. Bess, E. Chertova, J. Lifson, H. Grise, G. Ofek, K. Taylor, and K. H. Roux. 2006. Distribution and three-dimensional structure of AIDS virus envelope spikes. *Nature* 441: 847–852.
55. Sanchez-Martinez, S., M. Lorizate, H. Katinger, R. Kunert, G. Basanez, and J. L. Nieya. 2006. Specific phospholipid recognition by human immunodeficiency virus type-1 neutralizing anti-gp41 2F5 antibody. *FEBS Lett.* 580: 2395–2399.
56. Brunel, F., M. B. Zwick, R. Cardoso, J. Nelson, I. Wilson, D. Burton, and P. E. Dawson. 2006. Structure-function analysis of the epitope for 4E10, a broadly neutralizing human immunodeficiency virus type I antibody. *J. Virol.* 80: 1680–1787.